

Ultrasonic Inspection of Reconditioned Railroad Bearing Components – Year 1

Joseph A. Turner
Robert W. Brightfelt Professor of MME
Mechanical and Materials Engineering (MME)
University of Nebraska-Lincoln

Constantine Tarawneh
Director, UTCRS
Mechanical Engineering Department
University of Texas Rio Grande Valley

Sergio Martinez Jr.
Graduate Research Assistant
Mechanical and Materials Engineering
University of Nebraska-Lincoln

A Report on Research Sponsored by

University Transportation Center for Railway Safety (UTCRS)

University of Nebraska-Lincoln

September 2024

Technical Report Documentation Page

1. Report No. UTCRS-UNL-M2CY23	2. Government Accession No.	3. Recipient's Catalog No.	
4. Title and Subtitle Ultrasonic Inspection of Reconditioned Railroad Bearing Components – Year 1		5. Report Date September 30, 2024	
		6. Performing Organization Code UTCRS-UNL	
7. Author(s) Joseph A. Turner, Constantine Tarawneh, Sergio Martinez Jr.		8. Performing Organization Report No. UTCRS-UNL-M2CY23	
9. Performing Organization Name and Address University Transportation Center for Railway Safety (UTCRS) University of Nebraska-Lincoln (UNL) W342 Nebraska Hall Lincoln, NE 68588		10. Work Unit No. (TRAIS)	
		11. Contract or Grant No. 69A3552348340	
12. Sponsoring Agency Name and Address U.S. Department of Transportation (USDOT) University Transportation Centers Program 1200 New Jersey Ave. SE Washington, DC, 20590		13. Type of Report and Period Covered Project Report June 1, 2023 – August 31, 2024	
		14. Sponsoring Agency Code USDOT UTC Program	
15. Supplementary Notes This work is a collaborative effort between UNL, UTRGV, and MxV Rail			
16. Abstract Freight rail bearings are often subjected to heavy loads such that the performance of each bearing plays a crucial role in the safe operation of the entire train. Even bearings that are properly maintained may still fail due to rolling contact fatigue (RCF) if local regions within the bearing race do not meet established effective case depth (ECD) standards. In addition, little is known about potential changes that may occur within the highest stress region after extensive service life. Ultrasonic grain scattering shows sensitivity to both microstructure and residual stresses such that nondestructive measurement methods based on diffuse ultrasonic backscatter have shown a high correlation with the overall status of the raceway. Results from the first year showed clear differences between new and reconditioned bearing cups in terms of their ultrasonic signatures. This work will be expanded to include spatial maps of raceways to identify locations that are outside the statistical bounds expected for a given part. Those locations will be identified and those parts will be tested in simulated service life testing at UTRGV for comparison with the predictions.			
17. Key Words Bearings, Rolling Contact, Fatigue, Ultrasonic Tests, Microstructure, Residual Stress		18. Distribution Statement This report is available for download from https://www.utrgv.edu/railwaysafety/research/mechanical/index.htm	
19. Security Classification (of this report) None	20. Security Classification (of this page) None	21. No. of Pages 16	22. Price

Table of Contents

List of Figures	4
List of Tables	4
List of Abbreviations	4
Disclaimer	4
Acknowledgements	4
1. Introduction	5
2. Summary	5
3. Experiments	6
4. Spatial Statistics of the Ultrasonic Signals	10
5. Conclusions and Future Work	15
References	16

List of Figures

Figure 1. Diffuse ultrasonic scattering from near race of a cup.....	7
Figure 2. Photo of a bearing cup in the ultrasound immersion tank at UNL.	8
Figure 3. Ultrasonic C-scans from the top race of 5 cups including cup S with a large spall.....	9
Figure 4. Spatial variance curves for a few different cups.....	11
Figure 5. Upper and lower bounds of the magnitude of amplitude based on a Gumbel distribution.	13
Figure 6. Example outlier analysis based on bounds for cup S with the spall.....	14
Figure 7. An initial statistical analysis of the ultrasonic data.	15

List of Tables

No tables are included.

List of Abbreviations

American Railway Engineering and Maintenance-of-Way Association (AREMA)

Consolidated Rail Infrastructure and Safety Improvements (CRISI)

Effective Case Depth (ECD)

Federal Railroad Administration (FRA)

Rolling Contact Fatigue (RCF)

Disclaimer

The contents of this report reflect the views of the authors, who are responsible for the facts and the accuracy of the information presented herein. This document is disseminated under the sponsorship of the U.S. Department of Transportation's University Transportation Centers Program, in the interest of information exchange. The U.S. Government assumes no liability for the contents or use thereof.

Acknowledgements

The authors want to acknowledge the University Transportation Center for Railway Safety (UTCRS) at UTRGV for the financial support provided to perform this study through the USDOT UTC Program under Grant No. 69A3552348340. The authors also wish to acknowledge the in-kind contribution in terms of materials and time and effort provided by MxV Rail.

1. Introduction

A major goal of the UTCRS is devoted to a reduction in fatalities and overall accidents associated with rail transport. Railroad bearings under heavy loads must be manufactured to perform well over the course of the bearing lifetime which often exceeds one million miles [1]. In particular, the quality of the steel used for bearing production must ensure that mechanical behavior is consistent, especially in the regions of material subjected to the highest stresses. During service, bearings undergo rolling contact fatigue (RCF) and may fail due to subsurface fatigue spalls that result from micro-cracks initiated by near-surface defects acting as stress concentrators [2-4]. The production of high-quality steels has greatly reduced the probability of RCF failure, so new components rarely fail from RCF. However, little is known about the changes that may occur in the loaded regions of reconditioned bearings. The proposed research is focused on a new approach [5-6] to inspect reconditioned bearing components to identify and eliminate parts that may be susceptible to early failure.

2. Summary

The purpose of this project is to develop inspection metrics based on diffuse ultrasonic backscatter that can identify regions of reconditioned bearing components that may be more susceptible to early spalling. Compressive residual stresses are known to improve the service life of bearing components subjected to RCF. However, the correlation between the microstructure and stress state in raceways for deep case-hardened parts (i.e., depths > 0.050" or 1.27 mm) has not been quantified. The ability to quantify, map, and detect changes in raceways for every component would be transformative for railroad bearing safety. Current inspections of railroad bearing components are based on a visual inspection and comb detectors that identify surface defects such as spalls and pitting. This practice is an effective means to remove components from service or to recondition them for further use. However, these inspections do not assess the actual material state which is necessary to prevent crack initiation and to slow crack growth. Ultrasonic scattering has been used to detect impurities and inclusions in bearing steels and ultrasonic scattering can be used to quantify and predict the microstructural statistics of materials. Ultrasonic scattering is strongly linked with material microstructure and the state of residual stress within the test component [5-7]. Often, the scattering is assessed using diffuse ultrasonic backscatter for which the spatial

variance is the metric used to quantify scattering. The use of a focused transducer results in a measured spatial variance that is indicative of the focal properties of the transducer. The focus also enhances the scattering because of the concentration of energy within the focal zone. When combined with a model of the material microstructure, the peak of the spatial variance can be used to quantify microstructural statistics. Shear waves are generated using an oblique incidence measurement which nearly eliminates the front wall reflection. Thus, such an approach can be more sensitive to the changes in the near surface of raceways. For this project, research completed during the first year associated with measurements of the effective case depth with diffuse ultrasound will be used to develop inspection techniques that can be used to map regions of bearing parts that may have changed due to service loads. Once the inspection protocols are established, the approach will be used to identify locations with bearing components which are predicted to spall early.

3. Experiments

The initial experiments with bearing cups were based on prior results from Dr. Turner group through support of the FRA through the CRISI program. That work focused on the correlation between the diffuse ultrasonic backscatter and the effective case depth of bearing cones. Differences of the curvature of the raceway in cups and cones required updated measurement parameters. However, that work provided the basis for the best angle of incidence and focal depth to give clear shear spatial variance curves for cup races. A schematic of the cup race measurement is shown in Figure 1A. The amplitude profile shown in Figure 1B is typical of a shear backscatter measurement. The grain noise, the part of the signal of interest includes the initial reflection of the transducer side-lobe and then the scattering within the focal zone. Photos of the experimental configuration within the ultrasound immersion tank are shown in Figure 2. It should be noted that the transducer is mounted on a 90° angle mount so that the cup race can be accessed at the necessary oblique angle of incidence. During the scans, the cup rotates on the turntable and the transducer indexes up the race while maintaining a constant offset between the transducer face and the race.

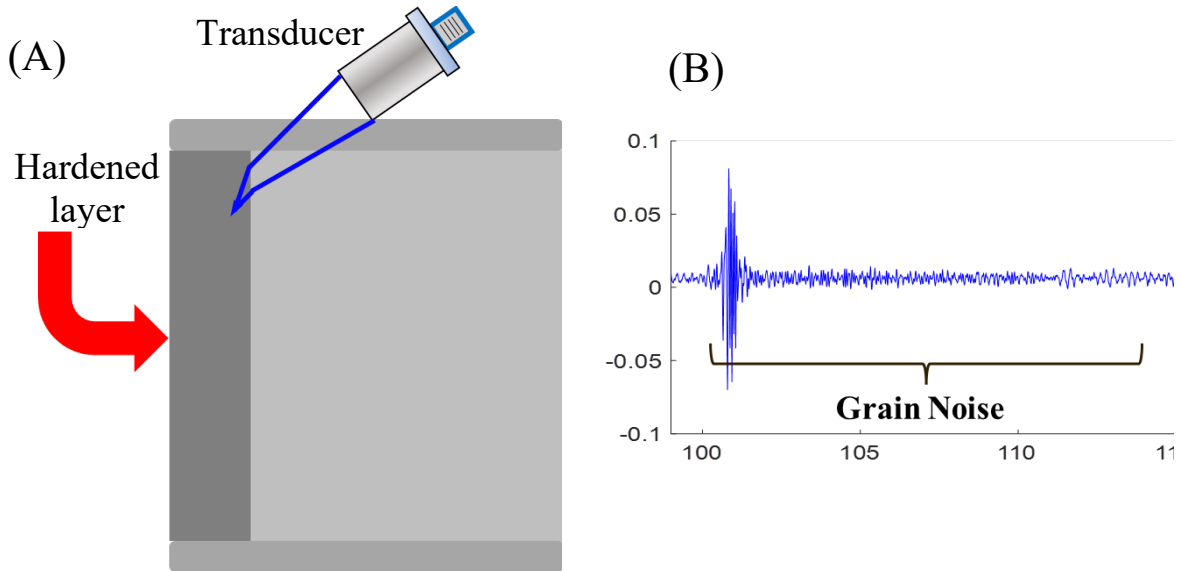


Figure 1. Diffuse ultrasonic scattering from near race of a cup.

The schematic shown in (A) shows the oblique angle of incidence used for the transducer in order to generate shear wave scattering within the hardened case depth of the cup. A typical grain noise signal, as shown in (B) represents the scattering from the grains within the focal zone.

During the experiments, an A-scan, such as that shown in Figure 1B, is collected at every spatial position. For each race, this data set includes ~31,000 signals. A C-scan is created by placing a gate on the signal to show the amplitude anywhere within the gate. A gate that captures the signal near the focal zone is used to highlight fundamental differences between the cups. C-scans from the top race of five cups are shown in Figure 3. Note that the high-amplitude signals that appear at the top of each race are due to strong reflections from the undercut and are not related to the material in the race. The trapezoidal shape of the C-scans is due to differences in the race circumference as a function of height that is the result of the cup taper. Cups A-D show clear differences in the shear scattering amplitude that are representative of the underlying grain structure of the cups. Cup C has the lowest overall scattering while cup D has many low-amplitude regions as well as numerous high-amplitude locations. Cups A and B have much higher scattering amplitudes with A having a more uniform scattering distribution. The large spall on cup S, Figure 3E, is visible but the amplitude is not meaningful because the rough surface is not amenable to a focused ultrasonic beam. Therefore, the region of the spall was not included in the subsequent signal statistics.

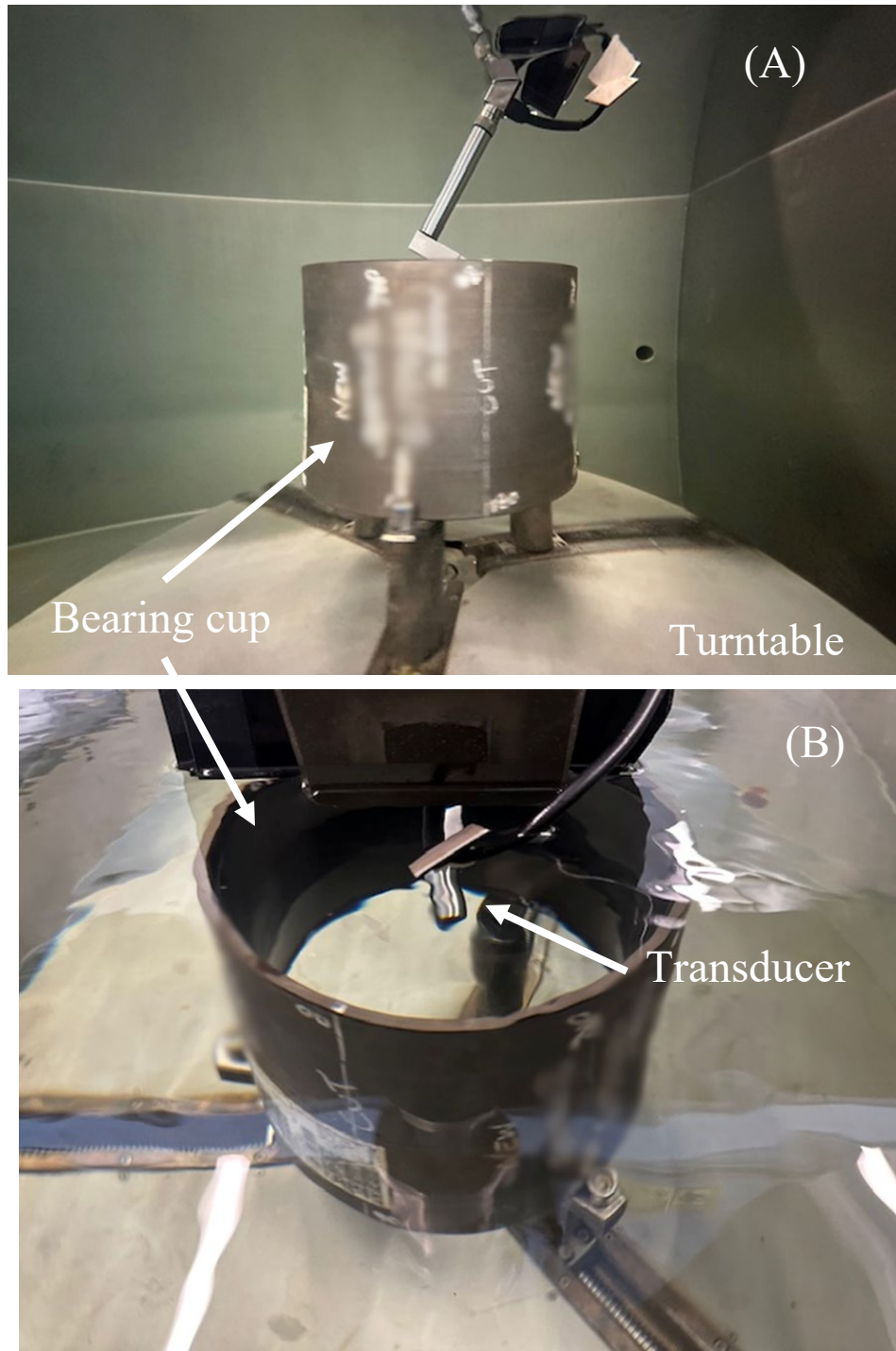


Figure 2. Photo of a bearing cup in the ultrasound immersion tank at UNL.

The transducer is connected with an L-fitting to allow for the oblique angle of incidence to be achieved within the interior of the cup. The side view in (A) shows the turntable and chucks used to hold the cup. The top view shown in (B) shows the 15 MHz focused transducer. During scans, the turntable rotates, and the transducer increments up the race.

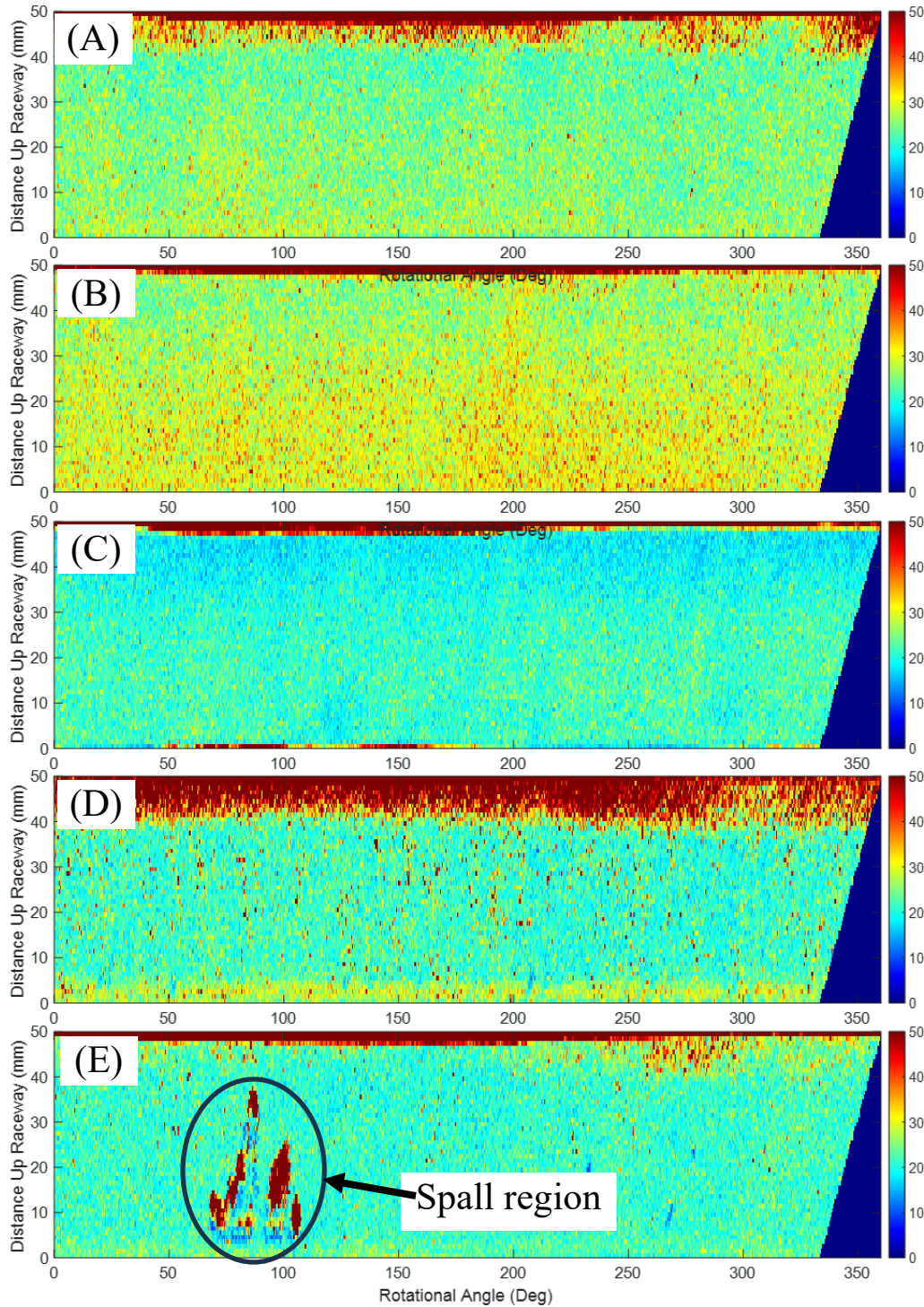


Figure 3. Ultrasonic C-scans from the top race of 5 cups including cup S with a large spall. The C-scans of the grain noise with a wide gate show large amplitude differences for each cup. Cups A-B shown in (A)-(B) have a higher scattering amplitude than cups C and D shown in (C) and (D). Cup S with the spall, shown in (E), has a background similar to cups C and D and the prominent spall region. Because of the taper of the raceway, the scans appear trapezoidal because the circumference of the race changes with height.

4. Spatial Statistics of the Ultrasonic Signals

The set of signals from each race includes about 31,000 amplitude scans similar to that show in Figure 1B. The goal of this project is to establish the statistical bounds for races of non-damaged cups so that the outliers can be identified and studied with respect to their potential for spalling. Using the ensemble of N signals from a given race, the spatial variance is calculated using

$$\Phi(\mathbf{t}) = \frac{1}{N} \sum_{i=1}^N [V_i(\mathbf{t}) - \bar{V}(\mathbf{t})]^2, \quad (1)$$

where $V_i(\mathbf{t})$ is the signal at the i th spatial position and $\bar{V}(\mathbf{t})$ is the mean of the ensemble of signals. With this definition, the spatial variance for a given race can be defined for any subset of the full ensemble. The spatial variance results for three cups are shown in Figure 4 for cups A, C, and S. Note that the variance for the top race of cup S does not include the region of the spall. The variance curves have a similar time dependence that resembles a skewed Gaussian. Such curves have also been observed for oblique incident shear wave backscatter in bearing cones [8]. The peak of the curves is approximately equal to the focal depth of the transducer. The skew in the backscatter is due to the oblique orientation of the transducer which insonifies the part surface with an elliptical focal area. The amplitude of the spatial variance curves is very similar for the top and bottom races of a given cup. However, the amplitude for each race is different and is correlated with the overall amplitude of the C-scans shown in Figure 3. In addition, the arrival time of the variance peak differs for each race. Our prior research with bearing cones showed a strong correlation between the peak arrival time and the effective case depth (ECD) [8]. The residual stress within the ECD changes the ultrasonic wave speed such that the scattered energy returns at different times. Perhaps more importantly, the measured spatial variance can be used to define the bounds within which the ensemble of signals is expected to lie. In this way, the probability that a given measurement position is outside the range of expectations can be assessed. The red portion of the signals shown in Figure 3 is the region of interest for the subsequent analysis. This range of time spans ~2-11 mm below the surface of the race.

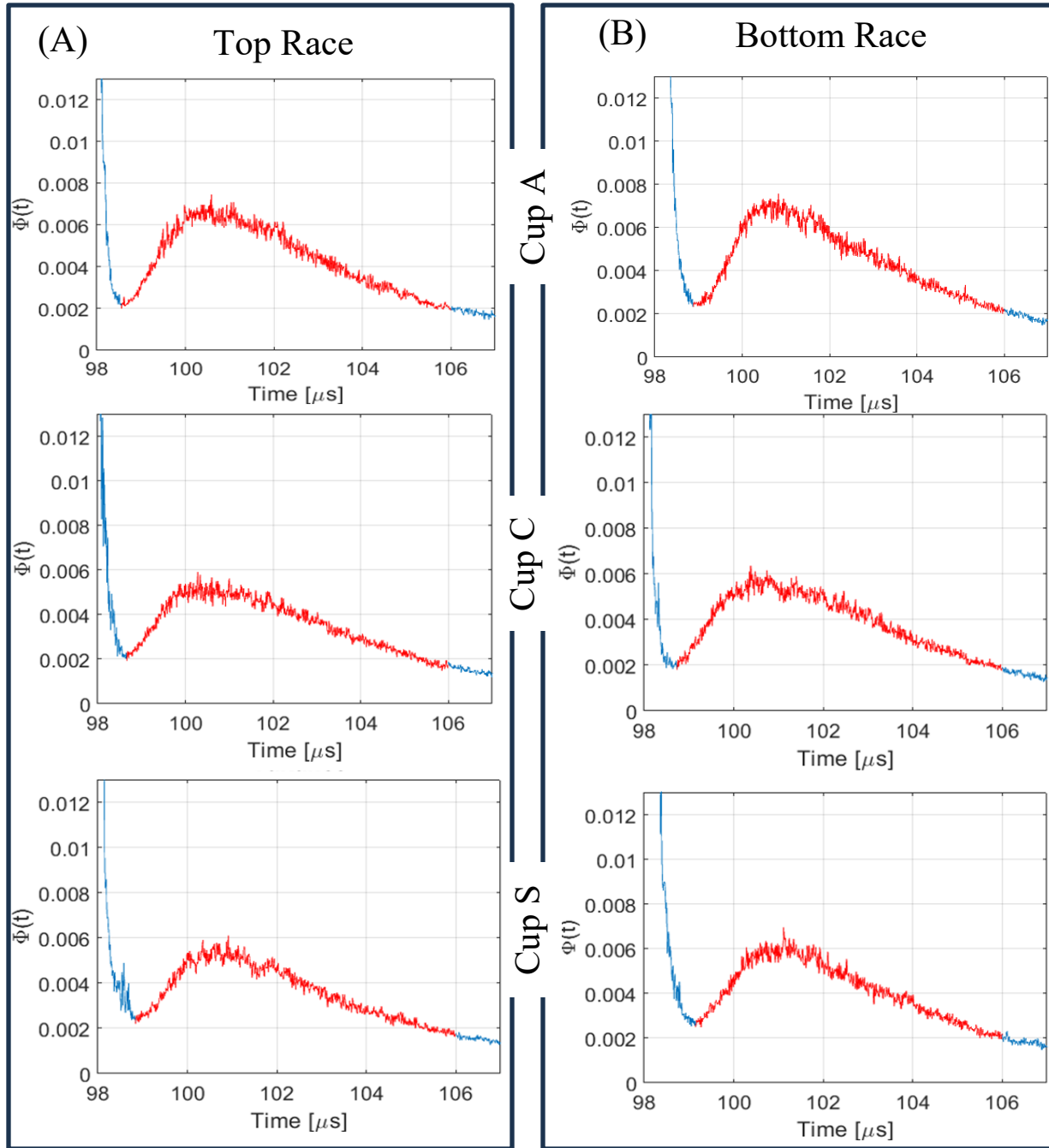


Figure 4. Spatial variance curves for a few different cups.

Results for the top races are shown on the left (A) while the results for the bottom races are shown in on the right (B) for cups A, C, and S. For all cups scanned, the results for the top and bottom races were very consistent for a given cup which reflects the steel and heat-treatment conditions.

Individual cups showed some differences such as cup A and C shown here. Note that the spall region of cup S was not used for the spatial variance calculation.

First, the signals are assumed to follow a Gumbel distribution [5]. In this case, the probability density function (PDF) for the signal $A(t)$ can be defined as

$$f_N(A(t)) = \frac{1}{a_N(t)} \exp \left\{ -\frac{A(t)-b_N(t)}{a_N(t)} - \exp \left[-\frac{A(t)-b_N(t)}{a_N(t)} \right] \right\}, \quad (2)$$

where

$$a_N(t) = \frac{\Sigma(t)}{\sqrt{2 \ln(N)}} \quad \text{and} \quad b_N(t) = \left[\sqrt{2 \ln(N)} - \frac{\ln(\ln(N)+\ln(\pi))}{2\sqrt{\ln(N)}} \right] \Sigma(t), \quad (3)$$

with $\Sigma(t)$ defining the standard deviation of the ensemble. With these definitions, the expected upper bound of the ensemble of signals can be defined as

$$U^{theory}(t) = \left[\sqrt{2 \ln(N)} - \frac{\ln \{ \ln(N) + \ln(\pi) + 2 \ln \left[-\ln \left(1 - \frac{1-\alpha}{2} \right) \right] \}}{2\sqrt{2 \ln(N)}} \right] \Sigma(t), \quad (4)$$

and the expected lower bound is given by

$$L^{theory}(t) = \left[\sqrt{2 \ln(N)} - \frac{\ln \{ \ln(N) + \ln(\pi) + 2 \ln \left[\frac{-\ln(1-\alpha)}{2} \right] \}}{2\sqrt{2 \ln(N)}} \right] \Sigma(t), \quad (5)$$

where $\gamma = 0.5772 \dots$ is the Euler-Mascheroni constant and α defines the confidence level. The bounds defined in Eqs. (4) and (5) are given in terms of the standard deviation which is related to the spatial variance by $\Sigma(t) = \sqrt{\Phi(t)}$. Thus, the bounds can be defined from a theoretical expression for the spatial variance [5] or from a measured region which is assumed to define the general statistics for the sample. This approach was used to define the appropriate bounds of the ultrasonic shear backscatter for regions of four raceways that showed a uniform scattering profile. These results are shown in Figure 5 for cups A and S using a 99.99% confidence bound for the analysis. With these bounds defined, every spatial position on the raceway can be evaluated to determine if the measured signal lies within the expected bounds.

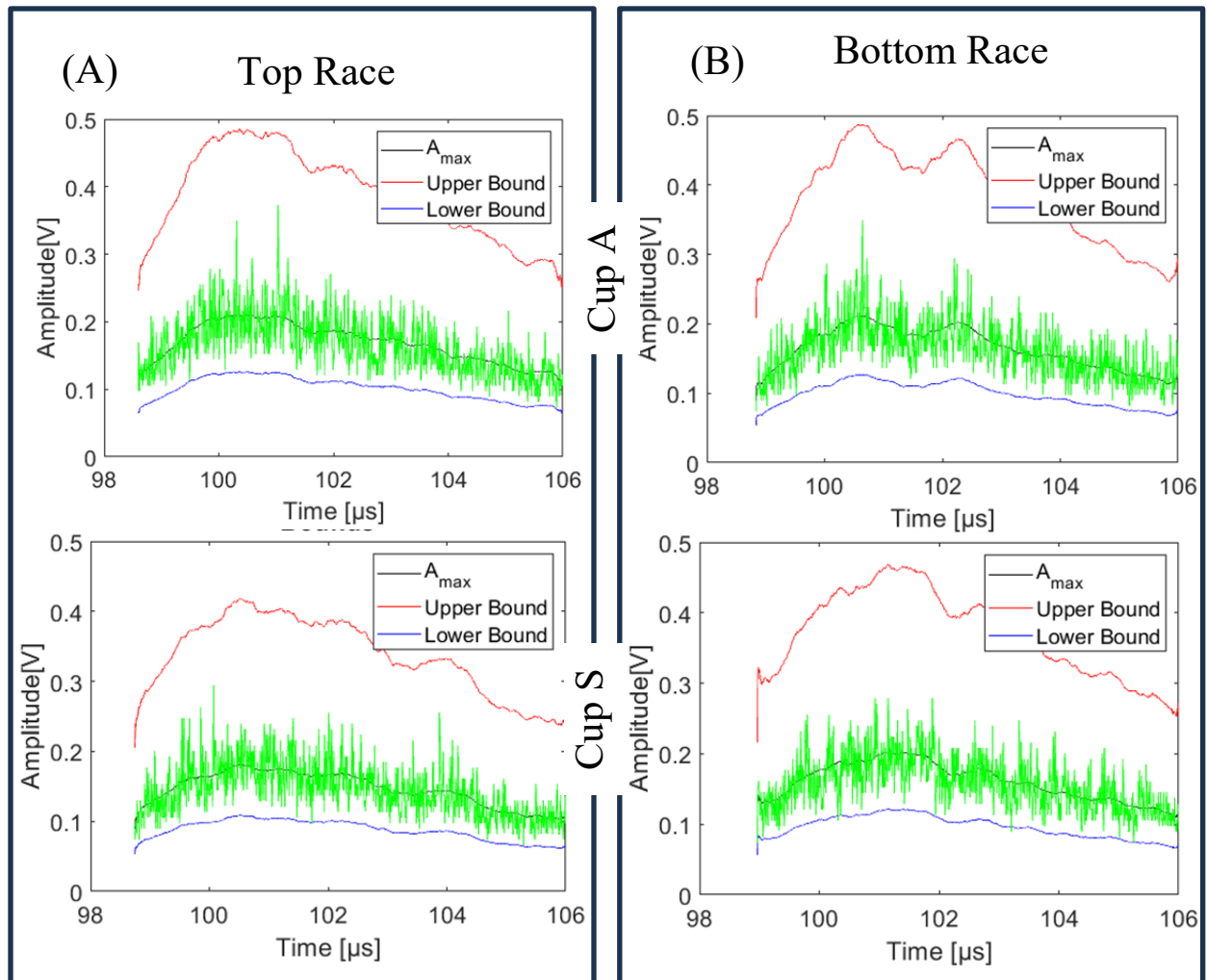


Figure 5. Upper and lower bounds of the magnitude of amplitude based on a Gumbel distribution. Regions of cup A and cup S were selected based on their noise profile. In this way, the nominal signal statistics can be defined.

Example results from this calculation are shown in Figure 6 for cup S using the race with the large spall. The overall results in Figure 6A show that the majority of pixels are blue which signifies that no part of the signal is above the upper bound. The insets for two pixels which are not blue are shown in Figure 6B-C. At these positions, the signal amplitudes are well above the upper bound which indicates a region of strong ultrasonic scattering. The arrival time of each peak identifies the approximate depth at which the scattering occurred. That depth is ~ 3.5 mm for Figure 6B and ~ 2 mm for Figure 6C. This analysis will continue for all cups.

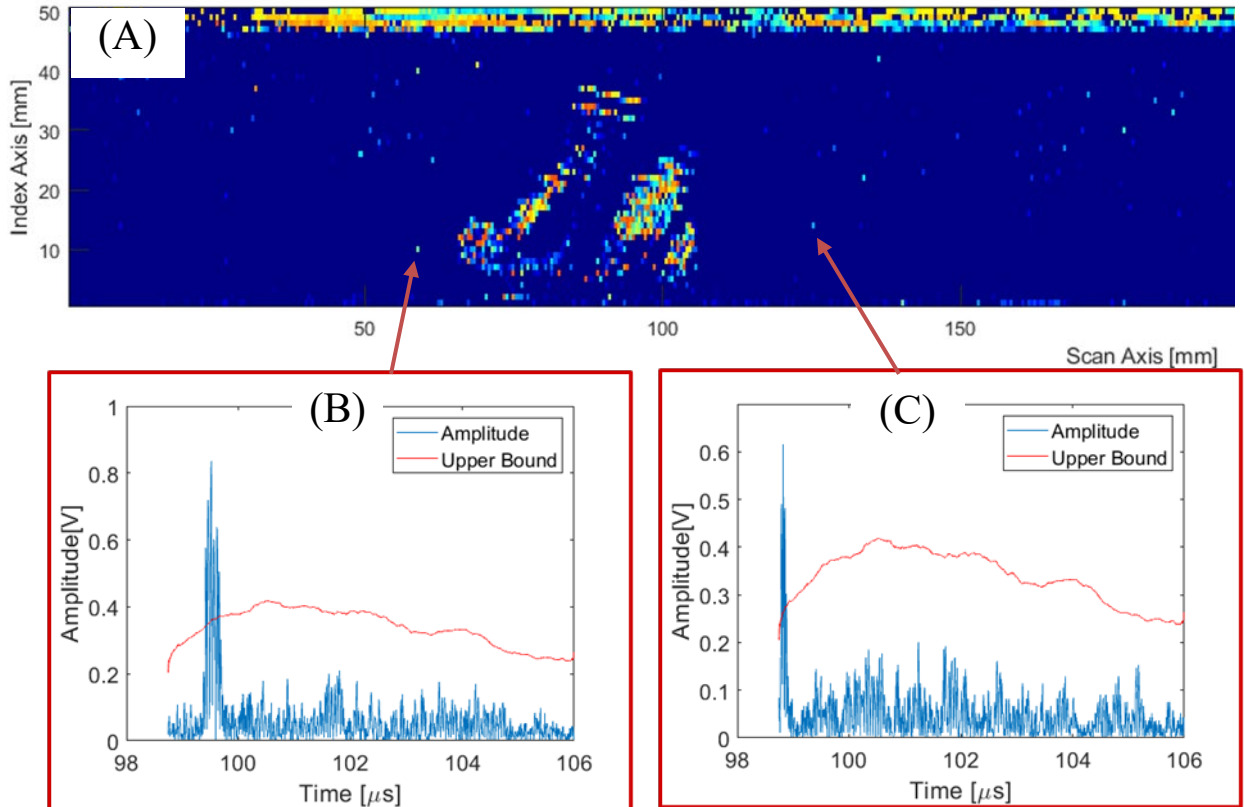


Figure 6. Example outlier analysis based on bounds for cup S with the spall.

The overall C-scan in (A) shows only pixels that have amplitudes above the 99.99% upper bound based on a ‘nominal’ area for this cup. Two example results for high-amplitude pixels are shown in (B) and (C). We hypothesize that the signals from these locations may indicate material that has subsurface microcracking or other material damage.

In addition, the specific characteristics of the ultrasonic signals are being studied in terms of their statistics. The model described above assumed that the signals follow a Gumbel distribution. That assumption must be tested before it can be used for further analysis. As an example, the statistics for a point in time at the beginning of the spatial variance curve are compared with three types of distributions, a normal distribution, a “t” location-scale distribution, and a logistic distribution. This comparison is shown in Figure 7 and it is clear that the “t” location-scale distribution fits best. Further comparisons with points along the entire window of the scattering profile must be examined. Once the statistics are defined, the outlier analysis can be expanded accordingly.

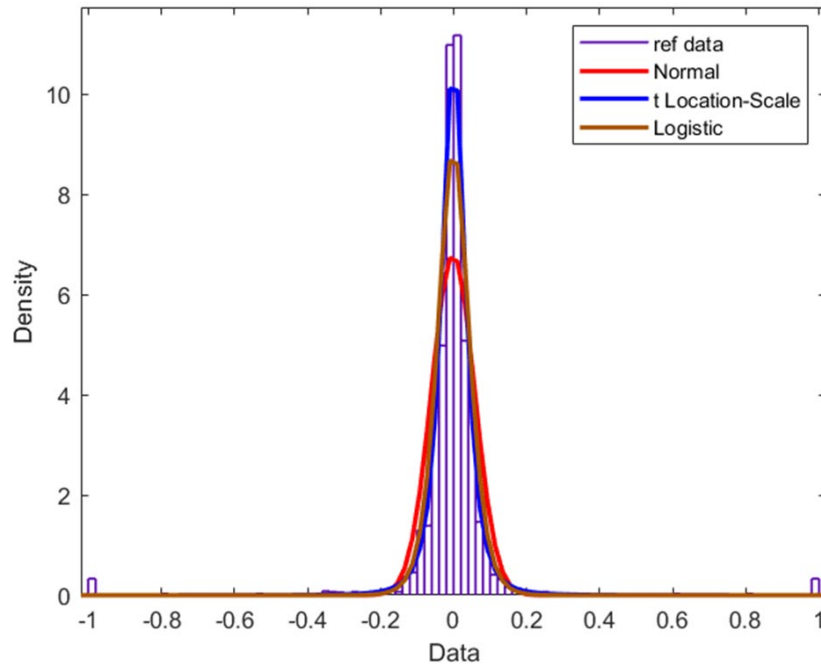


Figure 7. An initial statistical analysis of the ultrasonic data.

In this example, a single point in time is studied across the ensemble of ultrasonic signals for a single race. The statistics are examined with respect to different distribution types to determine which is best for further analysis. In this example, the t-location-scale fits much better than the normal or logistic distributions. Additional results will be generated for all cups that have been scanned and various time points in the signals.

5. Conclusions and Future Work

Initial experimental shear scattering measurements on railroad bearing cups show that the scattering behaves similarly to prior results on cones. The two raceways of a given cup show overall similar trends which suggests a uniform microstructure within a given part. At the same time, the differences in the grain noise profile are evident from each scan and the corresponding spatial variance profile. Statistical outlier analysis appears to have some value, but the full impact of these measurements will be known only during Year 2. During this time, simulated service life tests at UTRGV will be used and outliers will be placed within the highest stress region of the test fixture. This information will allow clear correlations to be created between the ultrasonic signatures and bearing fatigue life. Such information is critical to the safety of railroads.

References

- [1] C. Tarawneh, J. Montalvo, and B. Wilson, “Defect detection in freight railcar tapered-roller bearings using vibration techniques,” *Rail. Eng. Science*, vol. 29, no. 1, pp. 42–58, Mar. 2021, doi: 10.1007/s40534-020-00230-x.
- [2] F. Sadeghi, B. Jalalahmadi, T. S. Slack, N. Raje, and N. K. Arakere, “A Review of Rolling Contact Fatigue,” *Journal of Tribology*, vol. 131, no. 4, Sep. 2009, doi: 10.1115/1.3209132.
- [3] T. A. Harris and M. N. Kotzalas, *Advanced Concepts of Bearing Technology: Rolling Bearing Analysis*, Fifth Edition, 5th ed. Boca Raton: CRC Press, 2006. doi: 10.1201/9781420006582.
- [4] M. A. Mason, C. P. Cartin, P. Shahidi, M. W. Fetty, and B. M. Wilson, “Hertzian Contact Stress Modeling in Railway Bearings for Assorted Load Conditions and Geometries,” *Proceedings of the 2014 Joint Rail Conference*, Jun. 2014. doi: 10.1115/JRC2014-3846.
- [5] P. Hu and J. A. Turner, “Transverse-to-transverse (T-T) diffuse ultrasonic scattering,” *J. Acoust. Soc. Am.* 142, 1112-1120, 2017.
- [6] Y. Song, C. M. Kube, J. A. Turner, and X. Li “Statistics associated with the scattering of ultrasound from microstructure,” *Ultrasonics* 80, 58-61, 2017.
- [7] C. M. Kube and J. A. Turner, “Stress-dependent ultrasonic scattering in polycrystalline materials,” *J. Acoust. Soc. Am.* 139, 811-824, 2016.
- [8] T. Adelung, S. Islam, N. J. Matz, N. Swerczek, W. Brandl, A. J. Fuller, L. F. Ammerlaan, and J. A. Turner, “Dependence of Ultrasonic Scattering on Case Depth in Railroad Bearing Components,” *proceedings of the 31st ASNT Research Symposium*, Columbus, Ohio, June 26-30, 2023.